Polymer 50 (2009) 1124–1133

Contents lists available at ScienceDirect

Polymer

journal homepage: www.elsevier.com/locate/polymer

Synthesis and antimicrobial activity of quaternary ammonium-functionalized POSS (Q-POSS) and polysiloxane coatings containing Q-POSS

Partha Majumdar [a], Elizabeth Lee [a], Nathan Gubbins [a], Shane J. Stafslien [a], Justin Daniels [a], Clayton J. Thorson [a], Bret J. Chisholm [a,b,*]

[a] The Center for Nanoscale Science and Engineering, North Dakota State University, 1805 Research Park Drive, Fargo, ND 58102, USA
[b] Department of Coatings and Polymeric Materials, North Dakota State University, 1735 Research Park Drive, Fargo, ND 58102, USA

ARTICLE INFO

Article history:
Received 16 September 2008
Received in revised form
5 January 2009
Accepted 7 January 2009
Available online 14 January 2009

Keywords:
Polyhedral oligomeric silsesquioxane (POSS)
Polydimethylsiloxane
Antimicrobial

ABSTRACT

An array of quaternary ammonium-functionalized POSS (Q-POSS) compounds were synthesized and their antimicrobial properties toward the Gram-negative bacterium, *Escherichia coli*, and the Gram-positive bacterium, *Staphylococcus aureus*, determined in aqueous solution. Using Q-POSS compositions that exhibited broad spectrum antimicrobial activity in solution, the utility of the Q-POSS compounds as an antimicrobial additive for polysiloxane coatings was determined. The results of the investigation showed that Q-POSSs possessing a relatively low extent of quaternization and longer alkyl chain lengths provided the highest antimicrobial activity in solution. For polysiloxane coatings containing Q-POSS molecules as an antimicrobial additive, coating surface energy, surface morphology, and antimicrobial properties were found to be strongly dependent on Q-POSS composition. Coatings based on Q-POSSs possessing the lowest extent of quaternization displayed antimicrobial activity while analogous coatings produced using Q-POSSs possessing the highest extent of quaternization showed no antimicrobial activity. The lack of antimicrobial activity exhibited by coatings possessing Q-POSSs with a relatively high extent of quaternization was attributed to agglomeration of Q-POSS molecules through the formation of intermolecular interactions involving the quaternary ammonium moieties. Agglomeration would be expected to reduce diffusivity and inhibit interaction of the Q-POSS molecules with microbial cells.

1. Introduction

Silsesquioxanes, which have the general molecular formula $[RSiO_{1.5}]_n$ ($n \geq 4$), were first reported in 1946 by Scott [1]. Silsesquioxanes exist in a variety of structures among which polyhedral oligomeric silsesquioxane (POSS) compounds are of particular interest since they possess a unique cage-like structure and nanoscale dimensions (1–3 nm in diameter) [2]. Effective incorporation of POSS into a polymer matrix to produce a nanocomposite can result in increased glass transition temperature [3], enhanced mechanical properties [4,5], increased use temperature [6], lower flammability, and enhanced rheological properties [7]. Functionalized POSS with multiple reactive functionalities are ideal for the production of unique organic–inorganic hybrid nanomaterials. Functional groups such as epoxy [8,9], amine [10], vinyl [11], alcohol, carboxylic acid, fluoroalkyl, imide, and halide have been successfully incorporated into POSS structures and used for a variety of applications. Most of these functionalized POSS compounds are commercially available.

Quaternary ammonium compounds (QACs) are widely used as antimicrobial agents to inhibit microbial growth [12–15]. The antimicrobial activity provided by QACs results from both ionic and hydrophobic interactions between the QAC and components of the microbial cell wall that leads to cell death or malfunction in cellular processes [16–18]. The ability of a QAC to bind to the microbial cell wall and disrupt its function is dependent on various compositional factors such as charge density, amphiphilicity, molecular size, and molecular mobility. Since cell wall composition and structure varies from one microorganism to another, the effectiveness of a given QAC tends to vary from one microorganism to another. The complex relationship between QAC composition, microorganism species, and antimicrobial activity has been previously demonstrated by several investigators [19,20].

Traditionally, QACs containing one or two salt groups have been used as antimicrobial agents in commercial products; however, in nature, compounds containing multiple quaternary ammonium

* Corresponding author. The Center for Nanoscale Science and Engineering, North Dakota State University, 1805 Research Park Drive, Fargo, ND 58102, USA. Tel.: +1 701 231 5328; fax: +1 701 231 5325.
E-mail address: bret.chisholm@ndsu.edu (B.J. Chisholm).

0032-3861/$ – see front matter © 2009 Elsevier Ltd. All rights reserved.
doi:10.1016/j.polymer.2009.01.009

salt (QAS) groups are often used to inhibit biofilm formation [21,22]. As a result, QAS-functional polymers have been a subject of interest [23]. Compared to low molecular weight mono- or divalent QACs, QAS-functional polymers enable higher charge densities that provide higher affinities for the negatively charged microorganism cell wall. However, the higher molecular weight and higher extent of inter- and intramolecular ionic interactions associated with QAS-functional polymers inhibit diffusion through the cell membrane. As a means to enable high charge densities while maintaining a compact molecular structure, Chen et al. [24] investigated QAS-functional poly(propylene imine) dendrimers as an antimicrobial agent and showed that a dendrimer possessing 16 QAS groups per molecule provided two orders of magnitude greater antimicrobial activity than a monofunctional counterpart.

Since POSS molecules can be readily derivatized to possess as many as eight functional groups per molecule while maintaining a compact molecular size, it was of interest to synthesize quaternary ammonium functional-POSSs (Q-POSSs) and determine their antimicrobial activity as a function of the number of QAS groups per molecule. As previously discussed by Chojnowski et al. [25], Q-POSSs may also have utility as an antimicrobial additive for surface coatings. The excellent biocompatibility and desirable mechanical properties of polysiloxanes has resulted in numerous applications for these materials in the medical industry [26]. Since Q-POSSs possess a siloxane core that should enable compatibility with a siloxane matrix, they may be ideally suited as an antimicrobial additive for polysiloxane coatings.

This document describes the synthesis and antimicrobial activities of Q-POSSs possessing systematic variations in chemical composition. Antimicrobial activity of Q-POSSs in aqueous solution was determined using both the Gram-negative bacterium, *Escherichia coli* (*E. coli*), and the Gram-positive bacterium, *Staphylococcus aureus* (*S. aureus*). Q-POSSs exhibiting relatively high antimicrobial activity were subsequently incorporated into polysiloxane coatings and the antimicrobial activity of the coating surfaces determined using *E. coli*, *S. aureus*, and the opportunistic fungal pathogen, *Candida albicans* (*C. albicans*).

2. Experimental

2.1. Materials

Octasilane POSS was purchased from Hybrid Plastics. Allyldimethylamine was purchased from TCI America. Karstedt's catalyst (platinum(0)-1,3-divinyl-1,1,3,3-tetramethyl disiloxane complex), 1-iodomethane, 1-iodobutane, 1-iodooctane, 1-iodododecane, 1-iodohexadecane, 1-iodooctadecane, toluene, methanol, 1.0 M tetrabutylammonium fluoride (TBAF) in tetrahydrofuran (THF), 4-methyl-2-pentanone, and THF were obtained from Aldrich Chemical. 18,000 and 49,000 g/mol silanol-terminated polydimethylsiloxane (HO-PDMS-OH) and methyltriacetoxysilane (MeAc) were purchased from Gelest. Intergard 264 epoxy primer was obtained from International Marine and Protective Coatings. An 80 wt% solution of the 49,000 g/mol HO-PDMS-OH in toluene and a 50 mmol solution of TBAF in 4-methyl-2-pentanone (Cat soln.) were used for coating solution preparation. All other reagents were used as received.

For biological assays, tryptic soy broth (TSB), tryptic soy agar (TSA), Luria–Bertani broth (LBB), Luria–Bertani agar (LBA), Sabouraud's dextrose agar (SDA), yeast nitrogen broth (YNB), triphenyltetrazolium chloride, 10X phosphate-buffered saline (PBS), sodium chloride (NaCl), Dey–Engley neutralizing broth (D/E), HPLC grade methanol, 24-well polystyrene plates, 96-well polystyrene plates, and 1.5 ml centrifuge tubes were purchased from VWR International. 1X PBS was prepared in deionized water. 0.9% NaCl solution (w/v) was prepared by adding 9 g of NaCl to 1 l of deionized water.

Table 1
Quaternizing agent composition and weight used to quaternize 2.00 g of tertiary-amino-functional POSS.

Alkyl halide	High level of quaternization (wt in g)	Medium level of quaternization (wt in g)	Low level of quaternization (wt in g)
CH_3I	1.60	1.01	0.53
C_4H_9I	2.08	1.38	0.69
$C_8H_{17}I$	2.71	1.81	0.90
$C_{12}H_{25}I$	3.34	2.23	1.11
$C_{16}H_{33}I$	3.97	2.65	1.32
$C_{18}H_{37}I$	4.29	2.86	1.43

2.2. Q-POSS synthesis

A representative Q-POSS synthesis is as follows: In a 100 ml round-bottom flask equipped with a nitrogen inlet, condenser, and temperature controller, 2.00 g of octasilane POSS (1.96 mmol) and 1.75 g of allyldimethylamine (20.55 mmol) were dissolved in 50 ml of THF. Once dissolved, 180 μl of Karstedt's catalyst was added to the reaction mixture and the reaction mixture refluxed for 48 h. Completion of the reaction was confirmed using proton nuclear magnetic resonance spectroscopy (^{1}H NMR) by observing the disappearance of the Si–*H* peak at δ 4.7 ppm. After completion of the hydrosilylation reaction, excess allyldimethylamine was removed under reduced pressure. Allydimethylamine removal was confirmed by the absence of the ^{1}H NMR (in $CDCl_3$) peaks at δ 5.72 ppm (–N–CH_2–C*H*═) and 5.01 ppm (–N–CH_2–CH═C*H*$_2$). ^{29}Si NMR displayed a singlet at δ 14.9 ppm, corresponding to the M-type silicon, and another singlet at δ −107.3 ppm, corresponding to the Q-type silicon of the POSS core. The presence of only two singlets in the ^{29}Si NMR spectrum confirmed that the cubic structure of POSS remained intact during the reaction.

The tertiaryamino-functional POSS compound was converted to various Q-POSSs by quaternization using alkyl halides. A representative quaternization procedure is as follows: To a 20 ml glass vial containing a magnetic stir bar, 2.00 g of the tertiaryamino-functional POSS (9.4×10^{-3} mol of tertiary amine functional groups) was mixed with 0.90 g of 1-iodooctane (3.76×10^{-3} mol) and the quaternization reaction carried out at 50 °C for 48 h. A substantial increase in viscosity was observed as a result of the reaction. Using ^{1}H NMR (in $CDCl_3$), new peaks appeared at δ 3.5 ppm (–N^+–C*H*$_2$–) and 3.3 ppm [–N^+–(C*H*$_3$)$_2$] and a relative decrease of the dimethylamino protons at 2.2 ppm was observed. The extent of quaternization was approximately 40 mol%. Table 1 lists the composition and concentration of alkyl halides used to produce Q-POSSs while Table 2 provides the extent of quaternization obtained for each Q-POSS by ^{1}H NMR. Each Q-POSS was diluted with THF to produce a 30 percent solution by weight.

Table 2
Extent of quaternization obtained by ^{1}H NMR for each Q-POSS prepared. Values represent the mole percent of tertiary amines quaternized.

Alkyl halide	High level of quaternization	Medium level of quaternization	Low level of quaternization
CH_3I	63.5	42.3	18.9
C_4H_9I	95.1	76.4	37.6
$C_8H_{17}I$	90.5	76.9	39.7
$C_{12}H_{25}I$	94.5	71.1	37.0
$C_{16}H_{33}I$	82.9	65.6	38.2
$C_{18}H_{37}I$	81.7	66.9	38.9

Table 3
Compositions of the coatings produced (all values are in grams).

Coating	18K-HO-PDMS-OH	49K-HO-PDMS-OH	MeAc	Cat soln.	Q-POSS alkyl chain	Extent of Q-POSS quaternization	Wt of Q-POSS	Wt% of Q-POSS (based on 100 g of HO-PDMS-OH)	THF (from Q-POSS solution)	Toluene
18K-PDMS	7.00	0.00	1.05	1.05	–	–	0.00	0.00	0.00	0.00
18K-C12-QPOSS (low)	7.00	0.00	1.05	1.05	$C_{12}H_{25}$–	Low	1.16	16.57	2.71	0.00
18K-C16-QPOSS (low)	7.00	0.00	1.05	1.05	$C_{16}H_{33}$–	Low	1.24	17.71	2.89	0.00
18K-C16-QPOSS (high)	7.00	0.00	1.05	1.05	$C_{16}H_{33}$–	High	0.79	11.29	1.84	0.00
18K-C18-QPOSS (low)	7.00	0.00	1.05	1.05	$C_{18}H_{37}$–	Low	1.26	18.00	2.94	0.00
18K-C18-QPOSS (high)	7.00	0.00	1.05	1.05	$C_{18}H_{37}$–	High	0.83	11.89	1.94	0.00
49K-PDMS	0.00	7.00	1.05	1.05	–	–	0.00	0.00	0.00	1.75
49K-C12-QPOSS (low)	0.00	7.00	1.05	1.05	$C_{12}H_{25}$–	Low	1.16	16.57	2.71	1.75
49K-C16-QPOSS (low)	0.00	7.00	1.05	1.05	$C_{16}H_{33}$–	Low	1.24	17.71	2.89	1.75
49K-C16-QPOSS (high)	0.00	7.00	1.05	1.05	$C_{16}H_{33}$–	High	0.79	11.29	1.84	1.75
49K-C18-QPOSS (low)	0.00	7.00	1.05	1.05	$C_{18}H_{37}$–	Low	1.26	18.00	2.94	1.75
49K-C18-QPOSS (high)	0.00	7.00	1.05	1.05	$C_{18}H_{37}$–	High	0.83	11.89	1.94	1.75

2.3. Preparation of polysiloxane coatings

Coating solutions were prepared by adding HO-PDMS-OH, Q-POSS solution, and toluene to a 20 ml plastic cup and mixing at 2400 rpm for 2 min with a SpeedMixer™ DAC 150 FVE-K. Next, MeAc and Cat soln. were added to the mixture and the mixture mixed at 2400 rpm for an additional 2 min. The coating solutions were stirred overnight using magnetic stirring before applying the

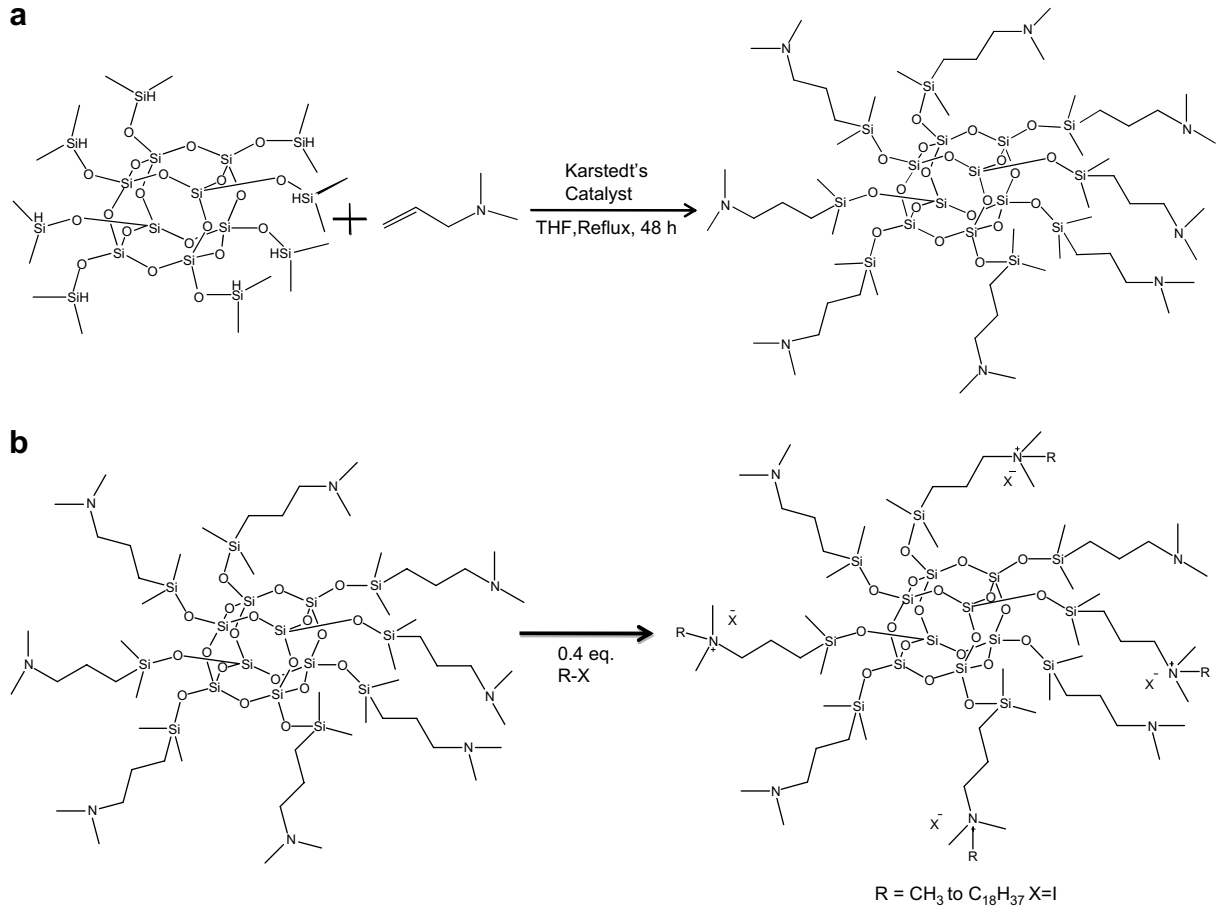

Fig. 1. (a) Synthesis of tertiaryamino-functionalized POSS. (b) An idealized structure of the partially quaternized Q-POSS.

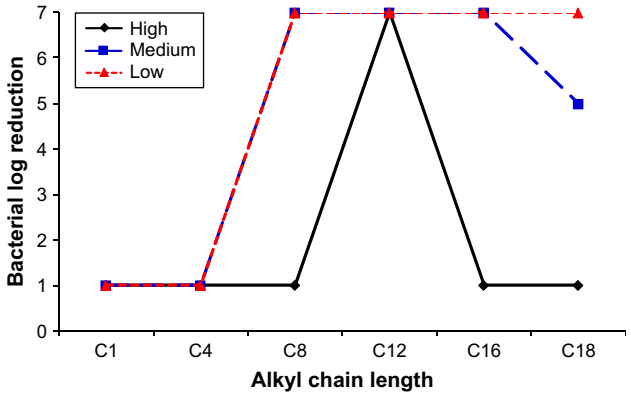

Fig. 2. A plot illustrating the antimicrobial activity of the Q-POSS compounds toward *E. coli* as a function of alkyl chain length and extent of quaternization (high, medium, and low).

coatings to substrates. Table 3 describes the compositions of the coating solutions prepared.

For the generation of coating specimens for antimicrobial testing, coating solutions were cast over primed aluminum discs using 200 μL of coating solution and an Eppendorf Repeater® plus pipetter. The primer used was Intergard 264 epoxy primer. For water contact angle measurements, drawdowns were made over aluminum panels by using a Gardco® applicator. Curing was achieved by allowing the coatings to lie horizontally for 24 h at ambient conditions followed by a 24 h heat treatment at 50 °C.

2.4. Antimicrobial property characterization of Q-POSSs

Stocks of *E. coli* ATCC 12435 and *S. aureus* ATCC 25923 were maintained weekly at 4 °C on LBA and TSB, respectively. Broth cultures of *E. coli* (LBB) and *S. aureus* (TSB) were prepared by inoculating one colony into 10 ml of broth and incubating at 37 °C with shaking. Overnight cultures were pelleted via centrifugation (10 min at 4500 rpm), washed twice in 0.9% NaCl, and resuspended to a 0.5 McFarland turbidity standard ($\sim 10^8$ cells ml^{-1}). 2 μl of 30 wt% Q-POSS in THF was added to 1 ml of bacterial suspension previously dispensed into a well of a sterile 24-well polystyrene plate. The plates were placed on an orbital shaker and allowed to incubate for 2 h at room temperature. 0.1 ml of each Q-POSS/bacterial suspension was immediately transferred to 0.9 ml of D/E neutralization medium in a 1.5 ml microcentrifuge tube, and serially diluted (1:10) in D/E medium. 0.2 ml of each dilution was

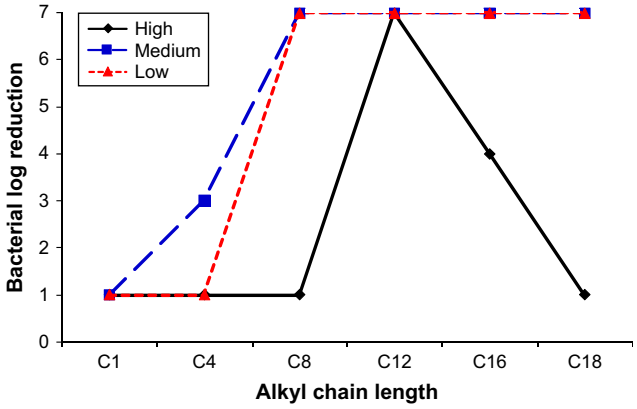

Fig. 3. A plot illustrating the antimicrobial activity of the Q-POSS compounds toward *S. aureus* as a function of alkyl chain length and extent of quaternization (high, medium, and low).

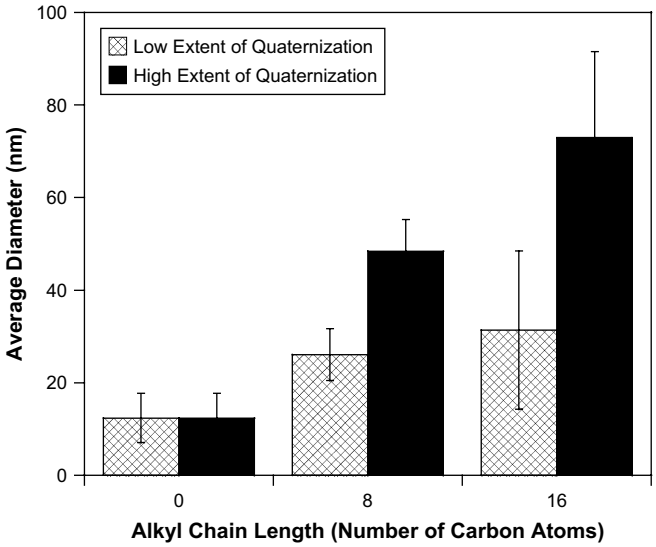

Fig. 4. Results of particle size measurements made on aqueous solutions of the tertiaryamino-functionalized POSS (0 carbon atoms) and Q-POSSs possessing an 8 or 16 carbon alkyl chain.

transferred in triplicate to a 96-well plate and incubated statically at 37 °C. After 24 h of incubation, the plates were removed from the incubator and photographed with a digital camera to quantify bacterial growth in solution. Bacterial log reductions were reported as the average of three replicate samples. The bacterial suspensions in 0.9% NaCl (without Q-POSS addition) served as a positive growth control (yellow color). Blank D/E medium served as the negative growth control (purple color). Since THF was used to solublize Q-POSS molecules for biological evaluations, the antimicrobial activity of THF was also determined. As expected, THF did not inhibit bacterial growth. Thus, variations in antimicrobial activity could be exclusively attributed to the Q-POSS molecules.

2.5. Antimicrobial property characterization of coatings containing Q-POSSs

The antimicrobial properties of coatings were determined using an agar plating method [27]. Stocks of *E. coli* ATCC 12435, *S. aureus* ATCC 25923, and *C. albicans* ATCC 10231 were maintained weekly at 4 °C on LBA, TSB, and SDA, respectively. Broth cultures of *E. coli* (LBB), *S. aureus* (TSB), and *C. albicans* (YNB) were prepared by inoculating one colony into 10 ml of broth and incubating at 37 °C with shaking. Overnight cultures were pelleted via centrifugation (10 min at 4500 rpm), washed twice in PBS, and resuspended to a final cell density of $\sim 10^8$ cells ml^{-1}. A sterile swab was used to inoculate a lawn of each microorganism on their corresponding agar plates. The coated aluminum discs were then placed on the agar plates with the coated side in direct contact with the agar surface. The plates were inverted and incubated for 24 h at 37 °C. Inhibition of microbial growth around and/or directly on the coating surfaces was evaluated visually from digital images taken after 24 h of incubation. A biological activity indicator dye, triphenyltetrazolium chloride, was added to the agar medium (70 mg/l *E. coli*, 15 mg/l *S. aureus*, 500 mg/l *C. albicans*) to aid in the visualization of microbial growth (i.e., red color).

2.6. Instrumentation

^{1}H NMR spectra were recorded in $CDCl_3$ using a JEOL 400 MHz spectrometer. A sweep width of 7503 Hz was used with 16,000 data

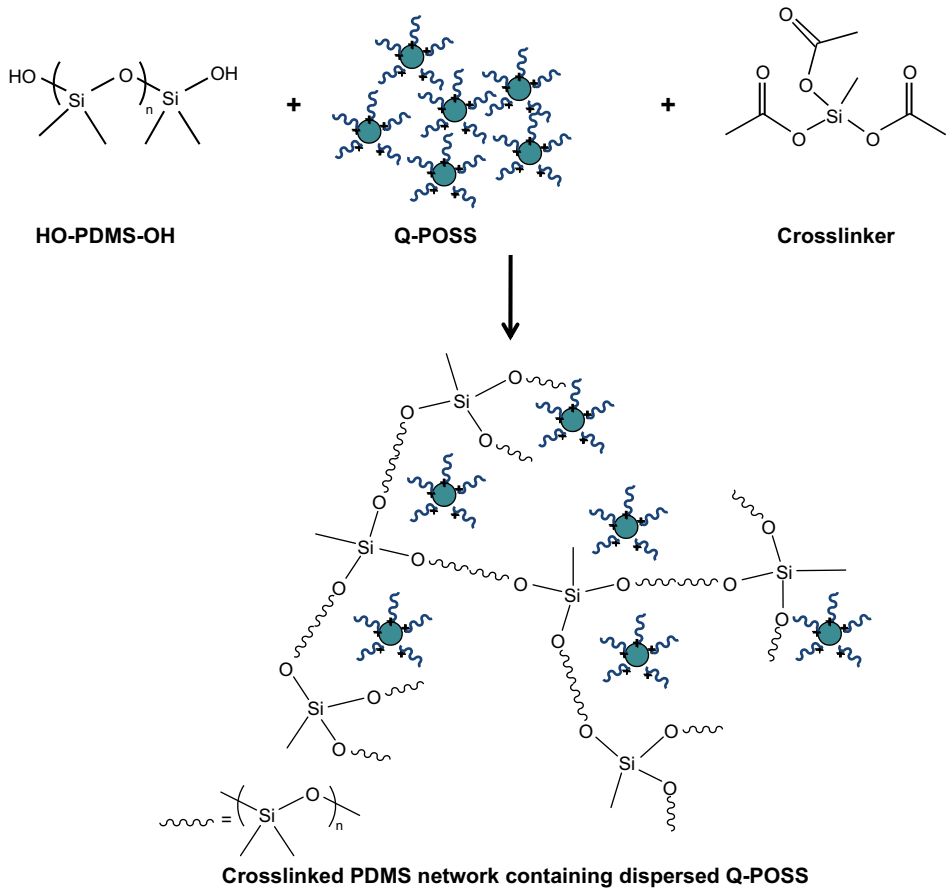

Fig. 5. A schematic representation of the crosslinked PDMS network containing dispersed Q-POSS molecules.

points, resulting in an acquisition time of 2.184 s. Sixteen scans were obtained with a relaxation delay of 4 s.

^{29}Si NMR spectra were collected using a JEOL 400 MHz spectrometer operating at 79.43 MHz. Acquisition parameters included a 62.5 kHz sweep width, 16,000 data points, and an acquisition time of 0.21 s. 14,000 scans were collected. The lock solvent was acetone-d_6 with chromium tris-acetyl acetonate added as a shiftless relaxation agent.

Water contact angle and water contact angle hysteresis were determined using an automated surface energy measurement unit manufactured by Symyx Discovery Tools, Incorporated [28]. For the determination of water contact angle hysteresis, advancing contact angle (θ_A) was measured by robotically adding water to a water droplet residing on the coating surface using an addition rate of 0.2 μl/s and monitoring changes in contact angle with time; while receding contact angle (θ_R) was measured by monitoring contact angle as water was withdrawn from the droplet using a withdrawal rate of 0.2 μl/s. The first image was taken after 20 s and subsequent images were taken every 10 s. The total duration of the water addition was 70 s as was the total duration of water removal. θ_A was determined by averaging the second to fifth data points during water addition while θ_R was determined by averaging the last four data points [29]. The difference between θ_A and θ_R was reported as the contact angle hysteresis.

Coating surface morphology was characterized using atomic force microscopy (AFM). The instrument utilized was a Dimension 3100® microscope with a Nanoscope IIIa controller from Veeco Incorporated. Experiments were carried out in tapping mode at

Table 4
Description of the coating variables investigated.

Variable	Level 1	Level 2	Level 3
HO-PDMS-OH molecular weight (g/mol)	18,000	49,000	–
Alkyl chain length	C12	C16	C18
Extent of Q-POSS quaternization	Low	High	–

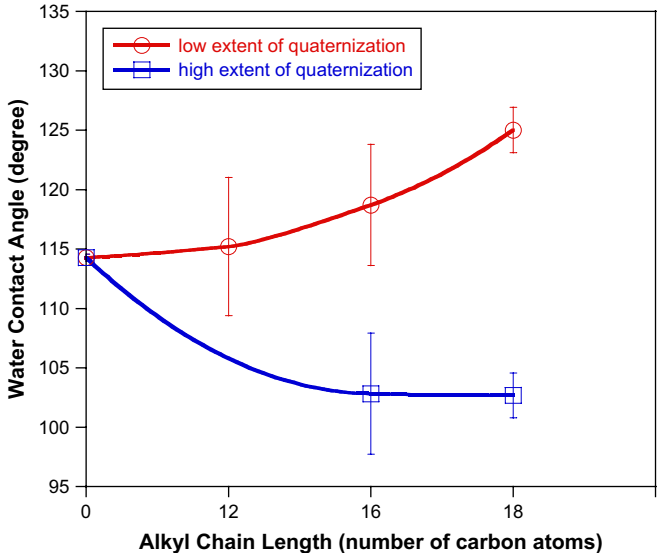

Fig. 6. Water contact angle data for coatings based on the 18,000 g/mol HO-PDMS-OH.

ambient conditions and both topographical and phase images were collected. A silicon probe with a spring constant of 0.1–0.4 N/m and resonant frequency of 17–24 kHz was used. The set point ratio for collection of images was 0.8–0.9.

Particle size measurements were obtained by dynamic light scattering with a Submicron Particle Sizer Nicomp™ 380 using a 658 nm laser and scattering angle of 90°. Samples were prepared by dissolving 2 μl of 30 wt% solutions of Q-POSS in THF in 1 ml of 0.9% NaCl (w/v in water). Three measurements were taken for each solution.

3. Results and discussion

As shown in Fig. 1, octasilane POSS was used as the starting compound to generate Q-POSSs. Octasilane POSS was chosen as the starting compound because the eight Si–H groups are a siloxane unit away from the inorganic cage resulting in a reduction in steric hindrance for further chemical modification [30]. As shown in Fig. 1(a), the first step of the Q-POSS synthesis involved hydrosilylation of octasilane POSS with allyldimethylamine to generate a functionalized POSS containing eight tertiaryamino groups. Complete functionalization was confirmed by ^{1}H NMR. ^{29}Si NMR was used to ensure that the cubic structure of POSS remained intact after the reaction.

The tertiaryamino-functionalized POSS was then used as a precursor to generate Q-POSSs. Quaternization of the tertiaryamino-functionalized POSS was achieved by reacting with iodoalkanes of varying chain length at 50 °C for 48 h. For each iodoalkane, the extent of quaternization was varied by varying the molar ratio of iodoalkane to dimethylamino groups at three different levels: high (1/1), medium (0.8/1), and low (0.4/1). The actual extent of quaternization achieved was determined by NMR and is provided in Table 2. With the exception of Q-POSSs generated from methyl iodide, the extent of quaternization was similar for a given level of iodoalkane.

3.1. Antimicrobial activity of Q-POSSs in aqueous solution

The antimicrobial activity of the Q-POSSs in aqueous solution was measured using the Gram-negative bacterium, *E. coli*, and the Gram-positive bacterium, *S. aureus*. Figs. 2 and 3 display antimicrobial activity of Q-POSSs as a function of both the length of the alkyl chain of the QAS groups and the extent of Q-POSS quaternization. Both alkyl chain length and extent of quaternization were found to significantly affect antimicrobial properties. In general, lower extents of quaternization and longer alkyl chain lengths provided the highest antimicrobial activity. For the highest extent of quaternization, antimicrobial activity exhibited a maximum at an alkyl chain length of 12 carbons.

Other investigators who have previously studied the antimicrobial properties of QACs have reported a strong dependence of antimicrobial properties on alkyl chain length. For example, Gilbert et al. [31] reported a parabolic relationship between the alkyl chain length of alkyltrimethylammonium bromides and antimicrobial activity toward *S. aureus*, *Saccharomyces cerevisiae*, and *Pseudomonas aeruginosa*. Maximum antimicrobial activity was observed for alkyltrimethylammonium bromides possessing 10 and 12 carbon alkyl chains. Similarly, Kourai and coworkers [32] observed a parabolic relationship between the alkyl chain length of *N*-alkyl-α-methylpyridinium iodides (MP), *N*-alkyldimethylphenylammonium iodides (dMPh), *N*-alkyltrimethylammonium iodides (tM), *N*-alkylquinolinium iodides (Q), and *N*-alkyl-*iso*-quinolinium iodides (IQ) and antimicrobial activity toward *E. coli* and *Bacillus subtilis* var. *niger*. For MP, dMPh, and IM, the 16 carbon-based QAC displayed the highest antimicrobial activity while the 14 carbon

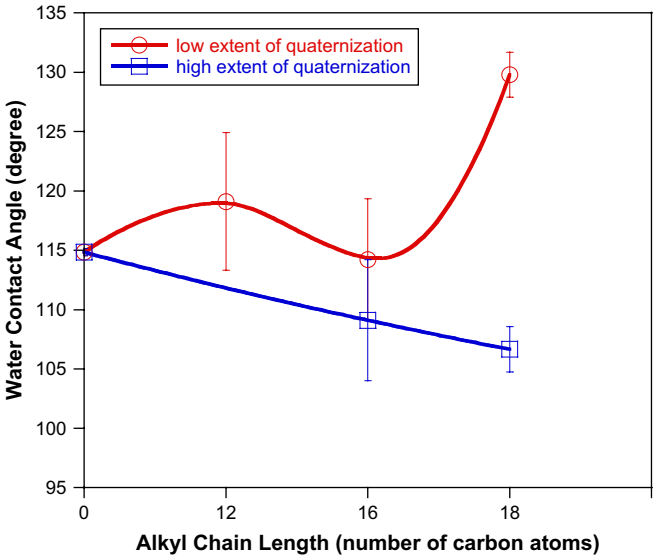

Fig. 7. Water contact angle data for coatings based on the 49,000 g/mol HO-PDMS-OH.

QAC was the most potent for Q and IQ. These nonlinear QAC chemical structure–antimicrobial activity relationships can be attributed to the interplay between several factors such as the affinity of the QAC for the cell membrane, the degree of aggregation of QAC or micelle formation of molecules in solution, steric interactions, and the diffusivity of the QAC through the cell wall [33–35]. The amphiphilic structure of QACs allows both the electrostatic and hydrophobic interactions needed to bind the biocide to the target organism cell wall [36,37].

Based on the data shown in Figs. 2 and 3, Q-POSSs possessing the lowest extent of quaternization and an alkyl chain length between 8 and 16 carbon units provided the highest, broadest spectrum antimicrobial activity. Apparently, Q-POSSs falling within this range of chemical structure possess the best balance of lipophilicity and diffusivity to enable both effective binding to the outer surface of the bacterium cell structure and diffusivity through the cell wall to the cell interior. It was hypothesized that the lower

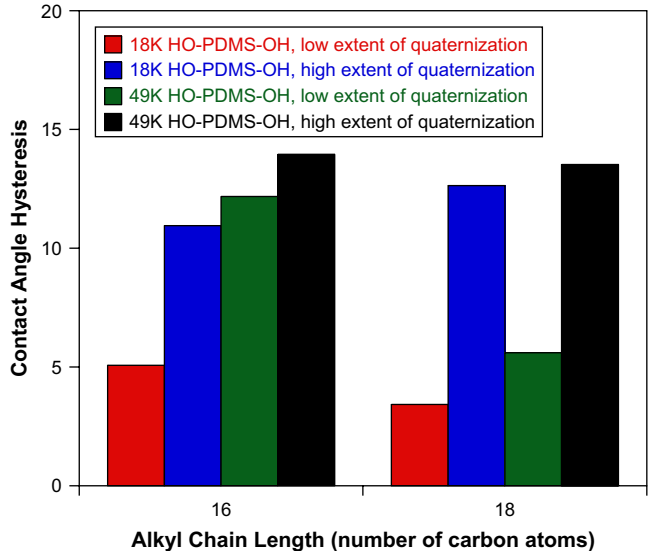

Fig. 8. Water contact angle hysteresis of coatings plotted as function of alkyl chain length and extent of quaternization of Q-POSS compounds.

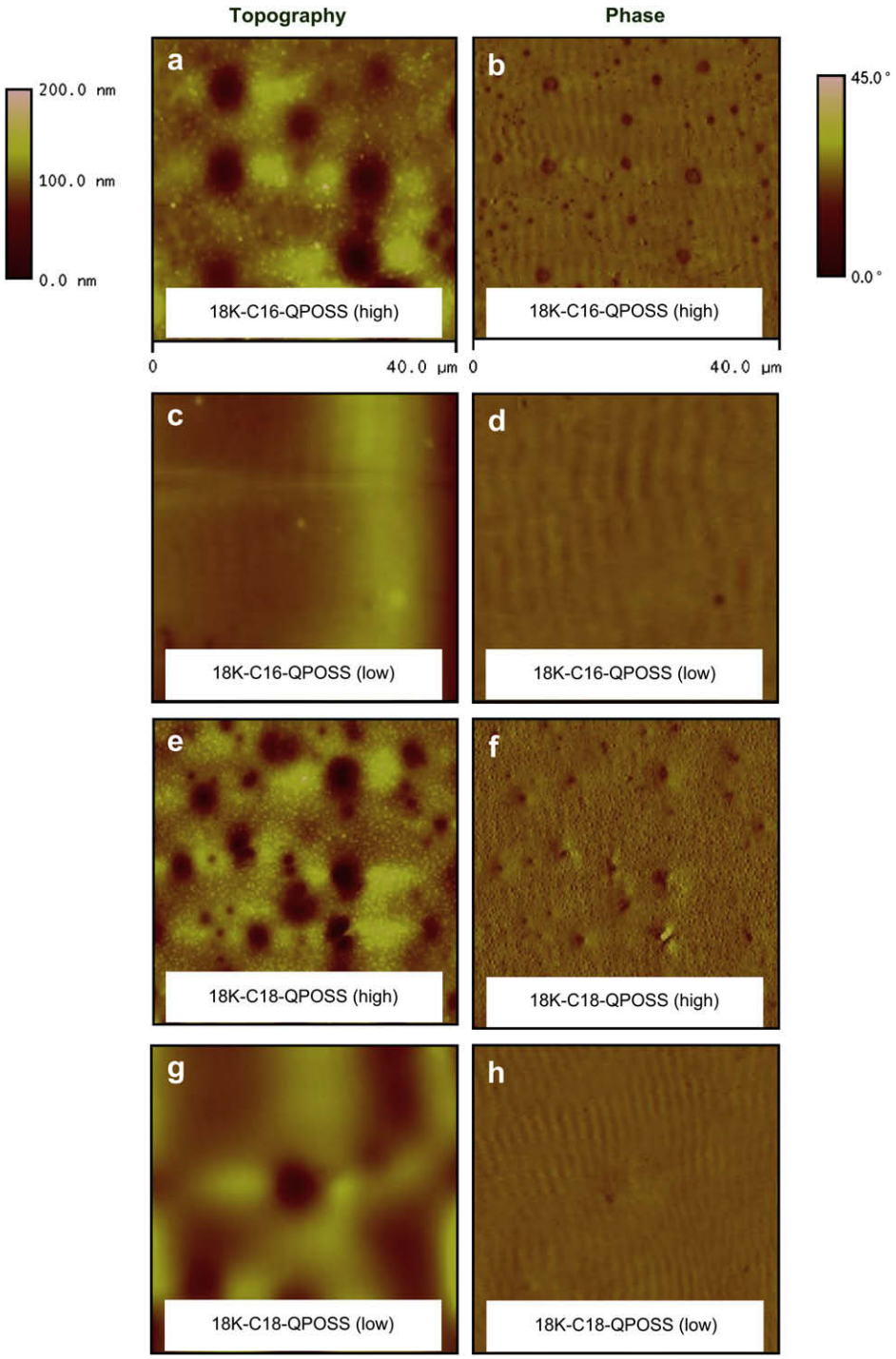

Fig. 9. AFM images of (a) 18K-C16-QPOSS (high), topography, (b) 18K-C16-QPOSS (high), phase, (c) 18K-C16-QPOSS (low), topography, (d) 18K-C16-QPOSS (low), phase, (e) 18K-C18-QPOSS (high), topography, (f) 18K-C18-QPOSS (high), phase, (g) 18K-C18-QPOSS (low), topography, and (h) 18K-C18-QPOSS (low).

effectiveness of Q-POSSs possessing the high level of quaternization may have been due to aggregation of Q-POSS molecules in solution which ultimately reduced the diffusivity needed to effectively permeate the cell outer layer and cause cell death. To test this hypothesis, particle size measurements of aqueous solutions of the tertiaryamino-functionalized POSS and representative Q-POSS samples were made using dynamic light scattering. The concentration of the solutions used for the measurement was the same as that used for measuring antimicrobial activity. As illustrated in Fig. 4, quaternization of the tertiaryamino-functionalized POSS resulted in a 2 to 6 fold increase in average particle size depending on the level of quaternization and alkyl chain length of the iodoalkane. Increasing the extent of quaternization from the low to the high level resulted in an approximate doubling of particle size. The changes in particle size resulting from quaternization can only be attributed to the formation of Q-POSS aggregates in the solution. The relatively large increase in average particle size observed as a function of alkyl chain length suggests that the driving force for

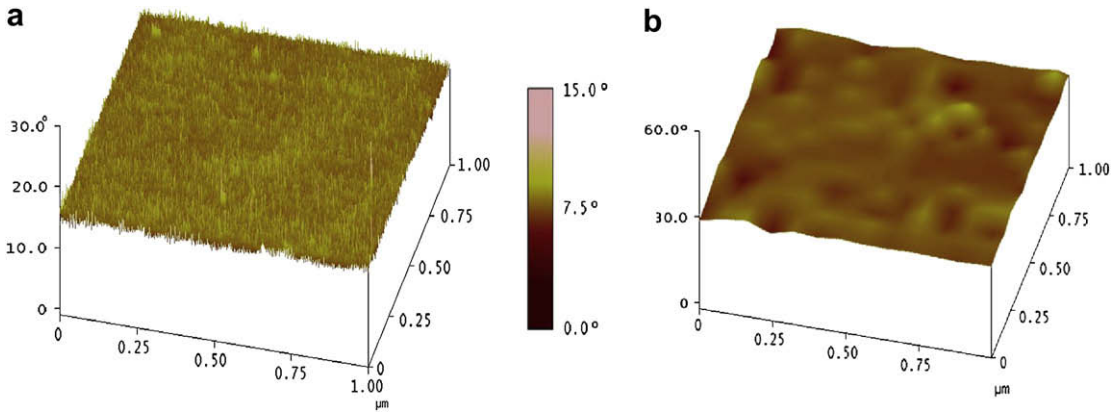

Fig. 10. AFM phase images of (a) 18K-C16-QPOSS (low) and (b) 18K-PDMS.

aggregation in aqueous solution was the formation of intermolecular hydrophobic interactions involving the long alkyl chains introduced into the POSS molecules via quaternization.

A variation in activity based on bacterial species was expected considering the significant differences in the cell wall of Gram-positive and Gram-negative bacteria. Gram-positive bacteria are generally characterized as having a thick cell wall composed of peptidoglycan and typically lack an outer membrane. Gram-negative bacteria are characterized as having a cell wall that consists of two membranes, an inner membrane based on phospholipids and an outer membrane composed of lipopolysaccharides [33,36]. Thus, for Gram-negative bacteria, the outer membrane of the cell wall acts as an additional barrier to foreign molecules. Previous results have shown that QACs tend to be more effective toward Gram-positive bacteria than Gram-negative bacteria [36,38]. However, the data shown in Figs. 2 and 3 show that, in general, Q-POSSs were just as effective toward the Gram-negative bacterium, *E. coli*, as the Gram-positive bacterium, *S. aureus*. The much higher charge density of Q-POSSs as compared to conventional QACs may have enabled the broader spectrum antimicrobial activity.

3.2. Surface properties of coatings containing Q-POSSs

After having identified Q-POSS compositions that exhibit broad spectrum antimicrobial activity, it was of interest to determine the utility of Q-POSSs as an antimicrobial additive for polysiloxane

Table 5
Illustrative examples of the antimicrobial responses observed for the coatings.

Microorganism	Antimicrobial responses observed		
	+, +	+, −	−, −
S. aureus			
E. coli	Not observed	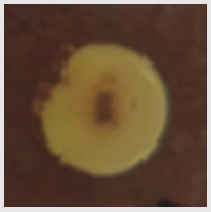	
C. albicans			

coatings. Considering the low surface free energy of polysiloxanes, it was of particular interest to determine if the more polar, and therefore higher surface energy, Q-POSSs would reside at the coating/air interface. Q-POSSs which varied with respect to the extent of quaternization and length of the QAS alkyl chain were incorporated into two different moisture-curable polysiloxane coatings and the coating surface properties characterized using water contact angle and water contact angle hysteresis measurements. The two moisture-curable polysiloxane coatings differed with respect to the molecular weight of the HO-PDMS-OH used to generate the crosslinked network. Fig. 5 provides a schematic representation of the crosslinked network produced by the coating solutions prepared. Table 4 provides a summary of the coating variables investigated.

Figs. 6 and 7 display water contact angle data as a function of both Q-POSS extent of quaternization and Q-POSS alkyl chain length. Interestingly, for both coating matrices (18K-PDMS and 49K-PDMS), adding Q-POSSs with a low extent of quaternization increased water contact angle while the opposite behavior was observed with the addition of Q-POSSs with a high extent of quaternization.

In addition to water contact angle, water contact angle hysteresis (CAH) was measured. CAH provides a measure of the stability of the coating surface upon exposure to water [39–41]. The results shown in Fig. 8 indicate that the use of Q-POSSs with a higher extent of quaternization results in a greater change in surface composition and/or morphology upon exposure to water. Considering the hydrophilicity associated with the QAS groups, it would be expected that increasing the extent of Q-POSS quaternization would result in a coating surface that would be more prone to undergo a rearrangement when exposed to the water droplet. The presence of water on the coating surface would provide a thermodynamic driving force for reorganization of QAS groups to maximize molecular interactions between QAS groups and water molecules.

AFM was used to characterize coating surface morphology as a function of Q-POSS extent of quaternization. The AFM images displayed in Fig. 9 were all obtained from coatings produced using the same HO-PDMS-OH (18,000 g/mol). A relatively homogeneous surface morphology was obtained for the coatings based on Q-POSSs with the low extent of quaternization [18K-C16-QPOSS (low) and 18K-C18-QPOSS (low)] while a relatively heterogeneous, two-phase surface morphology consisting of dispersed phases in the 2.0–4.5 μm size range was observed for the highly quaternized Q-POSS-based coatings [18K-C16-QPOSS (high) and 18K-C18-QPOSS (high)]. The micron-sized two-phase surface morphology observed for coatings based on the highly quaternized Q-POSS molecules indicates that the QAS groups provide a thermodynamic driving force for phase separation from the polysiloxane matrix. Most likely intermolecular ionic interactions such as those observed for "ionomers" are a principle factor in the formation of Q-POSS-rich domains [42]. In addition, intermolecular van der Waals interactions associated with the long QAS alkyl chains may also contribute to the driving force for phase separation.

Fig. 10 displays phase images of the pure PDMS matrix (18K-PDMS) and 18K-C16-QPOSS (low) taken at a much higher magnification than the images shown in Fig. 9. At the higher magnification (Fig. 10), it can be seen that the presence of Q-POSS produces a heterogeneous surface morphology at the nanometer scale indicating the presence of the Q-POSS molecules uniformly dispersed at the coating surface. The nanoscale surface topology observed from the Q-POSS (low)-containing coatings most likely contributed to the higher water contact angles observed for these coatings as compared to the Q-POSS-free coatings and Q-POSS (high)-containing coatings. The production of nanoscale surface roughness has been shown to reduce the contact area available for wetting which results in an increase in contact angle [43–45].

Table 6
Antimicrobial activity of coatings.

Coating	*S. aureus*	*E. coli*	*C. albicans*
18K-PDMS	−, −	−, −	−, −
18K-C12-QPOSS (low)	+, +	+, −	−, −
18K-C16-QPOSS (low)	+, −	−, −	+, +
18K-C16-QPOSS (high)	−, −	−, −	−, −
18K-C18-QPOSS (low)	−, −	−, −	+, −
18K-C18-QPOSS (high)	−, −	−, −	−, −
49K-PDMS	−, −	−, −	−, −
49K-C12-QPOSS (low)	+, −	−, −	+, −
49K-C16-QPOSS (low)	+, +	−, −	+, +
49K-C16-QPOSS (high)	−, −	−, −	−, −
49K-C18-QPOSS (low)	+, −	−, −	+, −
49K-C18-QPOSS (high)	−, −	−, −	−, −

3.3. Antimicrobial activity of coatings

The antimicrobial activity of the coatings described in Table 3 was evaluated toward the Gram-positive bacterium, *S. aureus*, Gram-negative bacterium, *E. coli*, and the opportunistic fungal pathogen, *C. albicans*, using the agar plating method. The antimicrobial properties of the coatings were characterized using visual observation. As illustrated in Table 5, three different antimicrobial responses were observed. For some coatings, no microorganism growth was observed on the surface of the coating or in a zone surrounding the coated specimen (zone of inhibition). This type of antimicrobial response was given the designation, "+, +." In addition to this response, coatings were identified that showed no microorganism growth on the coating surface, but no zone of inhibition. This antimicrobial response was given the designation, "+, −." Finally, coatings that showed no microorganism growth inhibition on the coating surface or a zone of inhibition were given the designation, "−, −."

Table 6 displays a summary of the results obtained from the agar plating method. In general, the Q-POSS-containing coatings were much more effective toward *S. aureus* and *C. albicans* than *E. coli*. Only coating 18K-C12-QPOSS (low) showed antimicrobial activity toward *E. coli*. Fig. 11 was generated using the data shown in Table 6 to enable visualization of the effects of the extent of Q-POSS quaternization and HO-PDMS-OH molecular weight on antimicrobial activity. Antimicrobial activity was represented as the number of microorganism species that were inhibited from growing on the coating surface. As shown in Fig. 11, only the coatings based on Q-POSSs that possessed the low extent of quaternization displayed

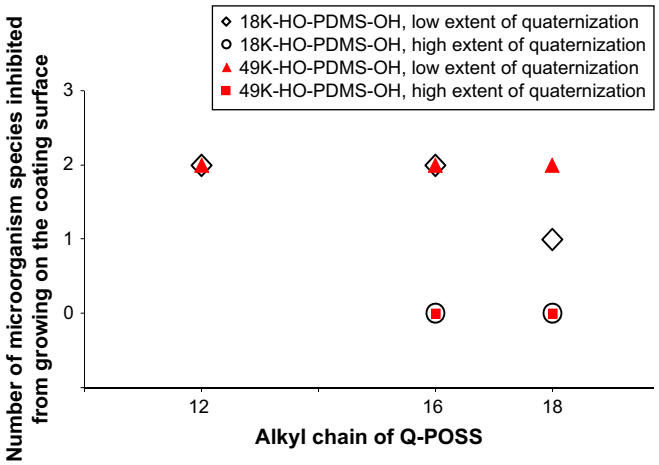

Fig. 11. The effects of the extent of Q-POSS quaternization and HO-PDMS-OH molecular weight on antimicrobial activity.

antimicrobial activity. The lack of antimicrobial activity for coatings doped with the highly quaternized Q-POSSs may be due to the extensive agglomeration of these Q-POSS molecules within the polysiloxane matrix that inhibits diffusivity of the Q-POSS molecules and thereby limits the ability of the molecules to interact with the cell wall of the microorganisms. As mentioned previously, the driving force for Q-POSS agglomerization most likely involved intermolecular interactions associated with the QAS groups. The formation of ionic aggregates in the solid-state for ion-containing polymers has been well documented [46–48]. Huang et al. has shown that QAS-functional polysiloxanes form ionic aggregates in the solid-state [42]. In addition to intermolecular ionic interactions, intermolecular van der Waals interactions associated with the long alkyl chain of the QAS groups may contribute to Q-POSS agglomerization. With regard to the effect of HO-PDMS-OH molecular weight on antimicrobial activity, the results shown in Fig. 11 indicate that this factor did not have an obvious effect on antimicrobial activity.

4. Conclusions

An array of Q-POSS compounds varying in the extent of quaternization and alkyl chain length were successfully synthesized. The antimicrobial activity of the Q-POSS compounds in aqueous solution was found to be strongly dependent on Q-POSS composition. In general, Q-POSSs possessing a relatively low extent of quaternization and longer alkyl chain lengths provided the highest antimicrobial activity. Based on particle size measurements of dilute aqueous solutions, the lower antimicrobial activity of Q-POSSs possessing a relatively high level of quaternization was attributed to Q-POSS aggregation in solution which inhibited diffusion into bacterial cell walls.

For polysiloxane coatings containing Q-POSS compounds as an antimicrobial additive, coating surface energy, surface morphology, and antimicrobial properties were found to be strongly dependent on Q-POSS composition. For coatings based on Q-POSS compounds possessing the low extent of quaternization, water contact angle was increased relative to analogous Q-POSS-free coatings and the coatings possessed nanoscale surface roughness not observed with the Q-POSS-free coatings. These results indicate that the Q-POSS molecules were present at the coating surface. For coatings based on Q-POSSs possessing the high extent of quaternization, a phase separated surface morphology was observed and water contact was lower than analogous Q-POSS-free coatings. The lower water contact angle and presence of a micron-scale dispersed phase at the coating surface suggested significant agglomerization of Q-POSS molecules for these coatings. In addition, coatings possessing the high level of quaternization did not display antimicrobial activity which may also be due to agglomerization of the Q-POSS molecules. Agglomeration of Q-POSS molecules resulting from extensive intermolecular ionic interactions and possibly intermolecular van der Waals interactions would be expected to inhibit diffusion and interaction of the Q-POSS molecules with bacterial cells. For coatings exhibiting a zone of inhibition, the zone of inhibition was quite small indicating low diffusivity of the Q-POSS molecules from the polysiloxane coatings into the agar medium.

Acknowledgement

The authors acknowledge financial support from the Office of Naval Research under grants N00014-05-1-0822 and N00014-06-1-0952.

References

[1] Scott DW. J Am Chem Soc 1946;68:356–8.
[2] Lligadas G, Ronda JC, Galia M, Cadiz V. Biomacromolecules 2006;7:3521–6.
[3] Seino M, Hayakawa T, Ishida Y, Kakimoto M. Macromolecules 2006; 39:8892–4.
[4] Pellice SA, Fasce DP, Williams RJ. J Polym Sci, Part B: Polym Phys 2003; 41:1451–61.
[5] Huang JC, He CB, Xiao Y, Mya KY, Dai J, Siow YP. Polymer 2003;44:4491–9.
[6] u HY, Kuo SW, Lee JY, Chang FC. Polymer 2002;43:5117–24.
[7] Fu BX, Namani M, Lee A. Polymer 2003;44:7739–47.
[8] Laine RM, Choi J, Lee I. Adv Mater 2001;13:800–3.
[9] Choi J, Harcup J, Yee AF, Zhu Q, Laine RM. J Am Chem Soc 2001;123: 11420–30.
[10] Tamaki R, Tanaka Y, Asuncion MZ, Choi J, Laine RM. J Am Chem Soc 2001; 123:12416–7.
[11] Zhang C, Babonneau F, Bonhomme C, Laine RM, Soles CL, Hristov HA, et al. J Am Chem Soc 1998;120:8380–91.
[12] Sauvet G, Fortuniak W, Kazmierski K, Chojnowski J. J Polym Sci, Part A: Polym Chem 2003;41:2939–48.
[13] Majumdar P, Lee E, Patel N, Stafslien SJ, Daniels J, Thorson CJ, et al. Polym Prepr (Am Chem Soc, Div Polym Chem) 2008;49(1):852–3.
[14] Stafslien SJ, Daniels JW, Majumdar P, Chisholm BJ. Polym Prepr (Am Chem Soc, Div Polym Chem) 2008;49(1):862–3.
[15] Sauvet G, Dupond S, Kazmierski K, Chojnowski J. J Appl Polym Sci 2000;75:1005–12.
[16] Donoruma LG, Vogl O. Polymeric drugs. New York: Academic Press; 1978.
[17] Davies A, Bentley M, Field BS. J Appl Bacteriol 1968;31:448–52.
[18] de Brabander-van den Berg EMM, Meijer EW. Angew Chem, Int Ed Engl 1993;32:1308–11.
[19] Gottenbos B, van der Mei HC, Klatter F, Nieuwenhuis P, Busscher HJ. Biomaterials 2002;23(6):1417–23.
[20] Gottenbos B, Busscher HJ, van der Mei HC, Nieuwenhuis P. J Mater Sci: Mater Med 2002;13(8):717–22.
[21] Mammen HC, Choi SK, Whitesides GM. Angew Chem, Int Ed 1998;37:2754–94.
[22] Sepcic K, Turk T. 3-Alkylpyridinium compounds as potential non-toxic antifouling agents. In: Muller WEG, editor. Marine molecular biotechnology. Germany: Springer; 2006. p. 105–24.
[23] Dizman B, Elasri MO, Mathias LJ. J Appl Polym Sci 2004;94:635–42.
[24] Chen CZ, Beck Tan NC, Cooper SL. J Chem Soc, Chem Commun 1999: 1585–6.
[25] Chojnowski J, Fortuniak W, Rosciszewski P, Werel W, Łukasiak J, Kamysz W, et al. J Inorg Organometal Polym Mater 2006;16(3):219–30.
[26] Ratner BD, Hoffman AS, Schoen FJ, Lemons JE, editors. Biomaterials science, an introduction to materials in medicine. 2nd ed. USA: Elsevier; 2004.
[27] Copello GJ, Teves S, Degrossi J, D'Aquino M, Desimone MF, Diaz LE. J Ind Microbiol Biotechnol 2006;33:343–8.
[28] Webster DC, Chisholm BJ, Stafslien SJ. Biofouling 2007;23(3):179–92.
[29] Majumdar P, Stafslien S, Daniels J, Webster DC. J Coat Technol Res 2007; 4(2):131–8.
[30] Neumann D, Fisher M, Tran L, Matisons JG. J Am Chem Soc 2002; 124(47):13998–9.
[31] Gilbert P, Al-Taae A. Lett Appl Microbiol 1985;1:101–4.
[32] Kourai H, Horie T, Takeichi K, Shibasaki I. J Antibact Antifung Agents 1980;8: 9–17.
[33] Chen CZ, Beck-Tan NC, Dhurjati P, van Dyk TK, LaRossa RA, Copper SL. Biomacromolecules 2000;1:473–80.
[34] Tashiro T. Macromol Mater Eng 2001;286:63–87.
[35] Juergensen L, Busnarda J, Caux PY, Kent RA. Environ Toxicol 2000;15(3): 174–200.
[36] Dubnickova M, Rezanka T, Koscova H. Folia Microbiol 2006;51(5):371–4.
[37] Walsh SE, Maillard JY, Russell AD, Catrenich CE, Charbonneau DL, Bartolo RG. J Appl Microbiol 2003;94:240–7.
[38] Ahlstrom B, Thompson RA, Edebo L. APMIS: Acta Pathol Microbiol Immunol Scand 1999;107:318–24.
[39] Schwartz LW, Garoff S. Langmuir 1985;1(2):219–30.
[40] Extrand CW, Kumagai Y. J Colloid Interface Sci 1996;184(1):191–200.
[41] Majumdar P, Lee E, Patel N, Ward K, Stafslien SJ, Daniels J, et al. Biofouling 2008;24(3):185–200.
[42] Huang Z, Yu Y, Huang Y. J Appl Polym Sci 2002;83:3099–104.
[43] Wenzel RN. Ind Eng Chem 1936;28(8):988–94.
[44] Lin T-S, Wu C-F, Hsieh C-T. Surf Coat Technol 2006;200:5253–8.
[45] Boduroglu S, Cetinkaya M, Dressick WJ, Singh A, Demirel MC. Langmuir 2007;23:11391–5.
[46] Taubert A, Wind JD, Paul DR, Koros WJ, Winey KI. Polymer 2003;44(6): 1881–92.
[47] Parent JS, Liskova A, Whitney RA, Resendes R. J Polym Sci, Part A: Polym Chem 2005;43(22):5671–9.
[48] Capek I. Adv Colloid Interface Sci 2004;112(1–3):1–29.